Res Chem Intermed (2011) 37:901–918
DOI 10.1007/s11164-011-0298-7

Selective solar photocatalytic oxidation of ethylbenzene on C, N, and S doped TiO_2

Basavaraju Srinivas · Police Anil Kumar Reddy · Mucharla Rajesh · Valluri Durga Kumari · Machiraju Subrahmanyam · Bhudev Ranjan De

Received: 3 January 2011 / Accepted: 15 February 2011 / Published online: 9 March 2011

Abstract The liquid-phase photo-oxidation of ethylbenzene (EB) is investigated in solar light with air/O_2/N_2 at atmospheric pressure, in a batch reactor using acetonitrile medium. It is carried out over TiO_2 doped with C, N, and S (TCNS) photocatalyst samples. The photocatalytic oxidation yielded acetophenone (33%) and 1-phenylethanol (21%) at 56% conversion of EB during a 6-h irradiation time. This product distribution indicates that C–H bond activation has occurred only at the alkyl chain. The effects of the EB to water content ratio, amount of photocatalyst and its sustainability, pH, have been studied. It is illustrated that the reaction carried out by this environmentally friendly photocatalysis is truly heterogeneous under mild conditions using solar light and no waste generation. An optimum loading of TCNS5 was observed for the photo-oxidation of EB.

Keywords Ethylbenzene oxidation · Acetophenone · Titanium dioxide · Photo-oxidation · C, N, and S doping

Introduction

The oxidation of benzyl C–H bonds constitutes one of the most fundamental transformations in organic synthesis. The aromatic ketones which are important chemical intermediates for the synthesis of various perfumes, drugs, and pharmaceuticals production are made by Frieda–Crafts acylation of aromatics by acyl halide or acid anhydride, using stoichiometric quantities of homogeneous acid. This

B. Srinivas · P. Anil Kumar Reddy · M. Rajesh · V. Durga Kumari · M. Subrahmanyam (✉)
Inorganic and Physical Chemistry Division, Indian Institute of Chemical Technology, Hyderabad 500607, India
e-mail: subrahmanyam@iict.res.in

B. R. De
Department of Chemistry and Chemical Technology, Vidyasagar University, Midnapur, India

leads to the formation of a large volume of toxic and corrosive wastes. Previously, efforts have been made to produce benzylic ketones by oxidizing the methylene group of alkyl aromatics using stoichiometric quantities of $KMnO_4$ as an oxidizing agent. However, in the above stoichiometric oxidation, the volume of waste produced is also very large, and separating reactants and products from the liquid reaction mixture is difficult.

In this context, the utilization of ethylbenzene (EB) in the xylene stream of the petrochemical industry to more value-added products is a worthwhile approach. In fact, the oxidation of EB has not drawn much attention due to the complexity of the products that could be formed. The reaction conditions are harsh, the product selectivity is poor, often corrosive promoters like bromide anions are used along with the catalyst, the separation of catalyst from the reaction mixture is difficult, the catalyst cannot be reused and also a lot of tarry waste is produced. It is, therefore, of great practical interest to develop a more efficient, easily separable, reusable, and environmentally friendly catalyst for this reaction. Processes based on oxidation, particularly replacing stoichiometric oxidation such as $KMnO_4$, Ag_2O, and CrO_3, by photocatalysis using solar energy at room temperature is, self-evidently, a sensible strategy to develop [1–6].

Photocatalytic organic synthesis arises from synthetic, mechanistic, or environmental application that represents a key strategy for the development of sustainable methods for chemical transformations [7, 8]. Reviews on the photocatalytic oxidation of various hydrocarbons are reported in the literature [9, 10]. Among the oxidation catalyst requirements, photoexcited semiconductors such as TiO_2 has attracted much attention in the last two decades. Semiconductor-mediated photocatalytic oxidation offers a facile and cheap method. Among various oxide semiconductor photocatalysts, TiO_2 has proved to be the most suitable catalyst for widespread environmental applications because of its biological and chemical inertness, strong oxidizing power, non-toxicity, and long-term stability against photo and chemical corrosion. However, the most negative property of TiO_2 is the need for using an UV wavelength of <387 nm (availability in solar light is $<5\%$), as the excitation source. In this context, we explored here the possibility to use TiO_2 anion-modified material in order to harvest a greater portion of solar radiation.

Several works reported that doping TiO_2 with anions such as carbon, nitrogen, sulphur, boron, and fluorine shifts the optical absorption edge of TiO_2 towards lower energy, thereby increasing the photocatalytic activity in the visible light region. Furthermore, DTA analysis studies reported on TiO_2 using thiourea as a precursor illustrates the role of dopant on the calcination temperature [11–14]. In the present investigation, the main focus is on shifting the absorption edge of TiO_2 to the visible light region by introducing C, N, and S into the TiO_2 lattice structure. The present results obtained provide a simple route for the preparation of C, N, and S doped TiO_2 with enhanced photocatalytic activity compared to bare TiO_2 under visible light irradiation for EB oxidation to acetophenone. To the best of our knowledge, no report is available in the literature on the photocatalytic oxidation of EB except for two, wherein in one report, environmental impact, high cost, and their hydrothermal and chemical stability are questionable issues [15] and the other one deals with UV-active TiO_2 alone with meager conversion and yields [16]. Based on these reports

and building on our previous expertise [7], we report herein the selective activation of benzylic C–H bonds of EB (difficult to oxidize due to the absence of an electron-donating aromatic ring-activation group) to acetophenone and 1-phenylethanol selectively using solar energy (Scheme 1).

The data obtained after 6 h of irradiation time and other optimization studies needed for any developmental work are reported in this paper.

Experimental

Materials and methods

All of the chemicals in the present work were of analytical grade and used as such without further purification. EB was of Fluka grade, titanium isopropoxide was from Sigma-Aldrich Chemie Munich, Germany, and acetonitrile (HPLC grade) was obtained from Ranbaxy Limited, India. All of the experiments were carried out with acetonitrile as the medium.

Preparation and characterization of catalyst

The catalyst samples for EB oxidation were C, N, and S doped TiO_2 prepared, characterized, and reported in our earlier paper using titanium isopropoxide as the precursor for titanium and thiourea as the source for carbon, nitrogen, and sulphur elements [11]. The weight (%) of thiourea doped TiO_2 was controlled at 0, 1, 3, 5, 10, 15, 25, and 40 wt% and the samples obtained were labeled as TCNS0, TCNS1, TCNS3, TCNS5, TCNS10, TCNS15, TCNS25, and TCNS40, respectively. All of the catalysts were characterized by techniques such XRD, XPS, and FTIR, SEM, BET surface area and UV–Vis DRS, CHNS elemental analysis [11].

Photocatalytic experiments

The substrate EB was taken in acetonitrile solvent. All of the photocatalytic experiments were carried out at the same concentrations until unless otherwise stated. Prior to illumination of the suspended solution, dark (adsorption) experiments were carried out for better adsorption of the EB on the catalyst. For solar

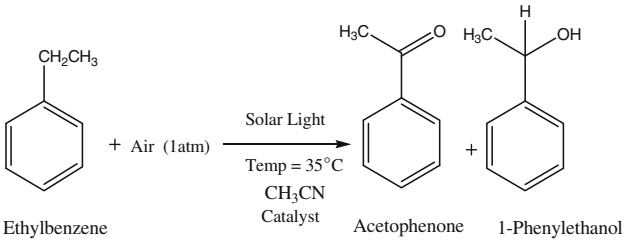

Scheme 1 EB oxidation over photocatalyst using solar irradiation

experiments, the EB solution of 2.73 × 10^{-2} M and the calculated amount of water was taken in a Borosil glass tube with a known amount of the catalyst sealed with Aldrich rubber septum. The solar photocatalytic experiments are conducted in a reactor wherein water was circulated around the reaction chamber, thus, maintaining the reaction at a constant temperature. The solar experiments were carried out during the time period 10.00 a.m. to 3.00 p.m. in May and June 2010 at Hyderabad, India.

Analysis

The EB oxidation was monitored by a Shimadzu SPD-20A HPLC system using a C-18 Phenomenex reverse-phase column with acetonitrile/water (70/30 v/v %) as the mobile phase at a flow rate of 1 mL min^{-1}. The samples were collected at regular intervals and filtered through Millipore microsyringe filters (0.2 μm).

Results and discussion

Characterization

BET surface area

The surface area of TCNS catalysts calcined at 400 °C is shown in Table 1. The high surface area of the prepared catalysts is due to the nano size of the particles. It is also observed that the surface area of the catalysts increases with the increase in the ratio of thiourea to TiO_2. This can be attributed to the decreasing of the particle sizes, as reported in the XRD analysis of the samples [11].

FTIR spectra

Figure 1 shows the FTIR spectra of TCNS0 and TCNS5 catalysts calcined at 400 °C. The absorption bands 2,800–3,500 and 1,600–1,680 cm^{-1} are assigned to the stretching vibration and bending vibration of the hydroxyl group respectively present on the surface of TiO_2 catalyst [17, 18]. The presence of surface hydroxyl groups are substantiated by XPS of O1s spectra [11]. The band around 1,730 cm^{-1}

Table 1 BET surface area and particle size of the TCNS catalysts

Catalyst	Particle size by XRD (nm)	BET surface area (m^2/g)
TCNS0	5.8	80.53
TCNS1	5.2	82.47
TCNS3	5.1	83.97
TCNS5	4.6	89.14
TCNS10	4.2	92.98
TCNS15	3.8	124.28

is attributed to the carbonyl group, and the bands at 1,130 and 1,040 cm^{-1} correspond to the nitrite and hyponitrite groups present in TCNS5 and they are absent in TCNS0, which shows the successful doping of nitrogen into the lattice of TiO_2 [11, 19, 20]. It is evident from the spectra that no peak corresponds to the NH_4^+ ion (absence of 3,189 and 1,400 cm^{-1}) in the prepared TCNS catalysts, which shows that N is present only in the form of nitrite and hyponitrite species [18].

SEM

The surface morphology of the TCNS photocatalyst is studied by SEM and the micrographs are presented in Fig. 2. The samples appear to be smaller particles. The SEM images of the TCNS0 (bare) and CNS-doped (TCNS5) catalysts showed that the particle morphology seems spherical in both of the images Fig. 2. The photograph of the TCNS5 sample exhibits well-dispersed particles and the particle is homogeneous with the formation of fine and well-dispersed particles. The investigation made for the sample used after the reaction (Fig. 2c) is illustrated later in recyclable activity studies. CHNS chemical analysis confirms that the amount of thiourea doped corresponds to 1% C, N, and S, which was observed for TCNS5. The higher activity on optimized reaction conditions of TCNS5, for the pre- and the post-reaction samples of TCNS5 chemical analysis showed 0.80–0.95% C, N, and S. This indicates that there were no surface changes on the catalysts after usage.

UV–Vis DRS

The UV–Vis diffuse reflectance spectra (DRS) of TCNS catalysts are shown in Fig. 3. It is seen from Fig. 3a that the undoped TiO_2 nanocatalyst (TCNS0) showed a strong absorption band around 380 nm in the UV region. But the TCNS sample showed absorbance at 400–470 nm, with band expansion (about 100 nm) towards the visible region. This expansion in the absorption edge decreases the direct band gap of TCNS catalyst compared to undoped TiO_2 (TCNS0) and this may be due to

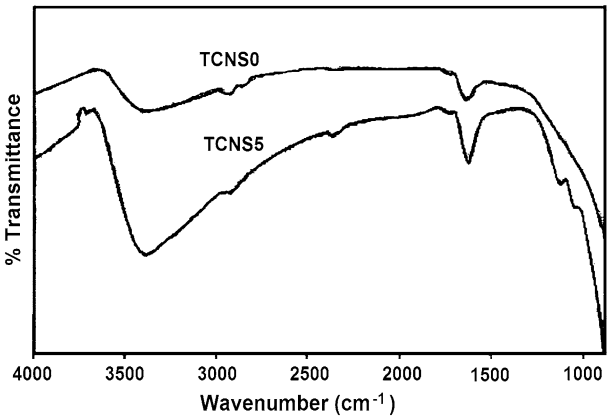

Fig. 1 FTIR spectra of TCNS catalysts

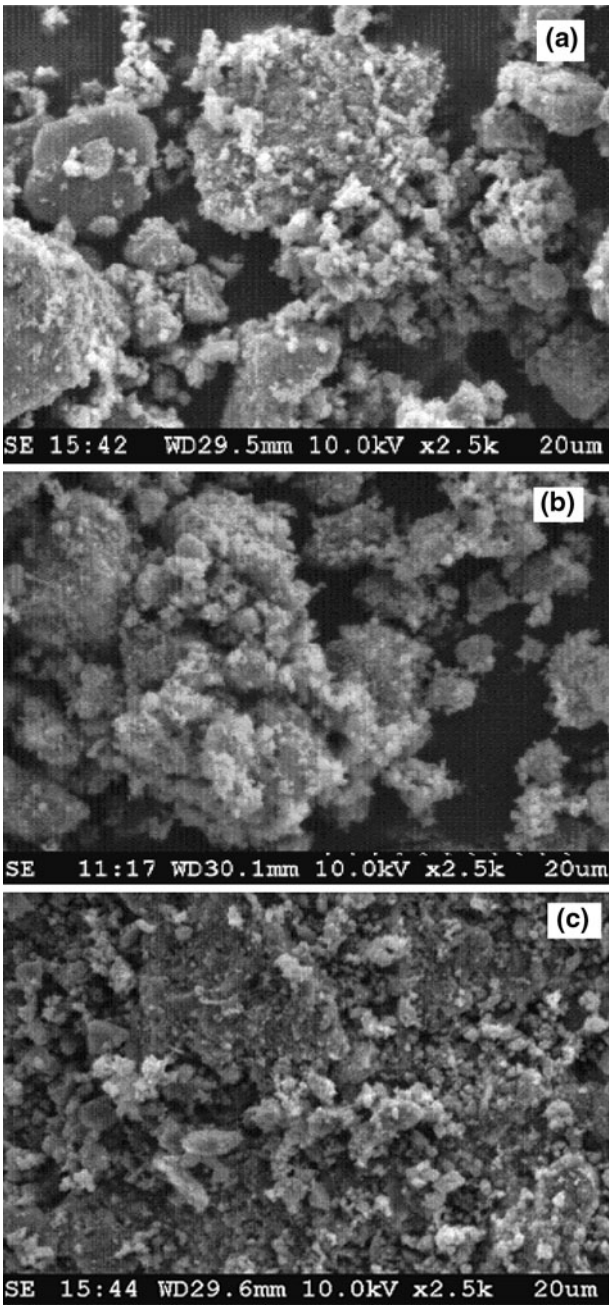

Fig. 2 SEM images of: **a** TCNS0 fresh, **b** TCNS5 fresh, and **c** used TCNS5

the insertion of C, N, and S into the TiO_2 lattice [14, 21, 22]. Furthermore, the band expansion in the DRS band increases with the increase in doped elements content into the TiO_2 lattice. The band gap energy (Eg value) of all of the catalysts is estimated from the plot of absorbance versus photon energy. The absorbance is extrapolated in order to obtain the band gap energy for the TCNS catalyst with good approximation, as observed in Fig. 3b. The estimated band gap energies of TCNS0, TCNS1, TCNS3, TCNS5, TCNS10, and TCNS15 are 3.05, 2.91, 2.82, 2.7, 2.6, and 2.41 eV, respectively. From the DRS results, it is clear that the C, N, and S doping

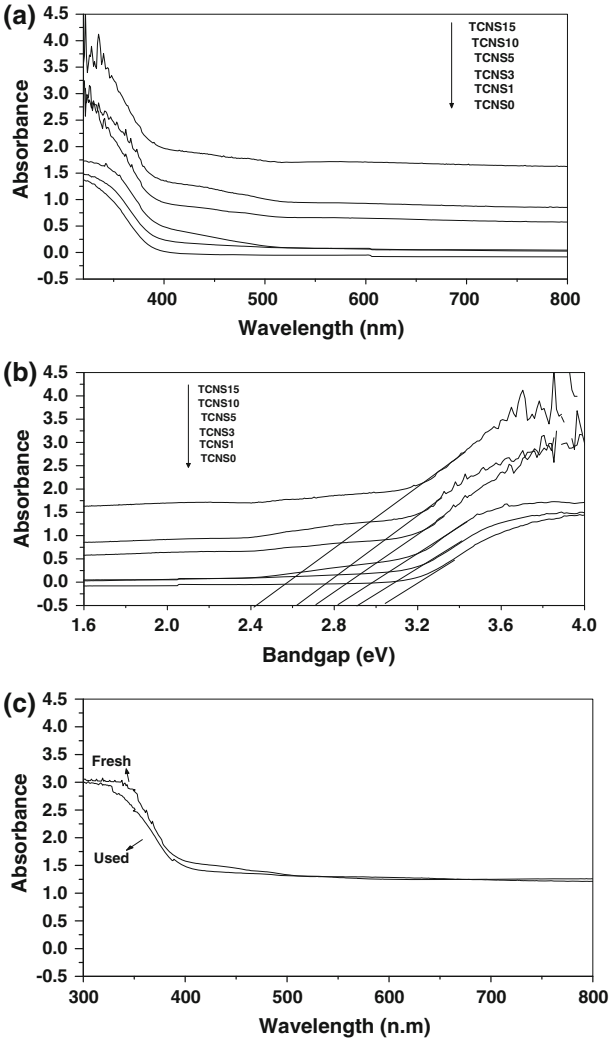

Fig. 3 UV–Vis DRS of TCNS catalyst samples: **a** absorbance versus wavelength of thiourea doped TiO_2, **b** absorbance versus band gap of thiourea doped TiO_2, **c** absorbance versus wavelength of TCNS5 fresh and used (third cycle)

can cause band expansion for the absorption of TiO_2 to the visible range and reduce the band gap, which is beneficial for improving the photoabsorption and, ultimately, the photocatalytic performance of TiO_2.

XPS

To investigate the chemical states of the possible dopants incorporated into TiO_2, Ti2p, O1s, C1s, N1s, and S2p binding energies are studied by measuring the XPS spectra [11].

Photocatalytic activity

Prior to the photocatalytic experiments, adsorption and photolysis studies were carried out. The EB solution was kept in the dark without catalyst for one day and no oxidation is observed. 3.33 g L^{-1} of the catalyst in 2.73 $\times$ 10^{-2} M of EB in acetonitrile solution is kept in the dark. Aliquots were withdrawn at regular intervals and the observation of no change in EB concentration indicates no adsorption of the substrate on the catalysts prepared. The photolysis (without catalyst) experiment is carried out under the solar light, taking 2.73 $\times$ 10^{-2} M of EB solution in the Borosil glass tube and only 2% conversion was observed, with no desired product even after 6 h of solar irradiation.

Selection of catalyst

To compare the TiO_2 photocatalytic oxidation of EB activity of the commercial P25 and lab-made TiO_2 (sol–gel method) samples and also CNS doped TiO_2 (lab-made) activity, evaluation runs were carried out under solar light irradiation.

All of the studies are carried out at 3 g L^{-1} catalyst amount in 2.73 $\times$ 10^{-2} M EB in acetonitrile solution, keeping the molar ratio of EB to water as 5.4. The photocatalytic activity of TCNS catalysts under solar light irradiation is shown in Table 2. Among all of the samples, TCNS5 photocatalyst showed better activity. The activity increased gradually with the increasing amount of dopent, and it reached an optimum of 5 wt% loading of C, N, and S and any further increase resulted in an activity decrease with time. The photocatalytic activity of the samples can be attributed to the following factors. The work reported from our studies [11] and others [23–25] regarding the doping of C, N, and S elements in titanium dioxide results in visible light absorption spectral response in the photocatalytic samples and the same is observed from the UV-DRS (Fig. 3). It can be seen from the DRS spectra that C, N, and S doping resulted in an intense increase in absorption in the visible light region and the absorption expansion of the base material titania (Fig. 3a, b). The band-gap narrowing of titania by C, N, and S doping lead to enhanced photocatalytic activity of the titania under visible light. But we can also see that, at higher loadings, the photocatalytic activity of TCNS samples decreased, though they showed greater red shift in the absorption expansion. It might be due to the fact that the excess dopent acts as recombination centers which facilitates electron–hole recombination, thus, lowering the activity. So, the photocatalytic

activity is depressed to a certain extent. To conclude, the higher activity of the TCNS5 sample can be ascribed to the high surface area, strong adsorption in the visible region, and lower recombination of electron–hole pairs due to the high concentration of surface hydroxyl groups, which can trap the photogenerated holes and, thus, decrease the electron–hole recombination process.

Effect of illumination time on EB oxidation over TCNS5

In order to further study the process, the influence of reaction time on the catalytic performance is illustrated in (Fig. 4). As the time progresses, the conversion of EB is increased and reached a maximum of 56% by 12 h and, after that, no change in concentration is noted due to the surface coverage of EB and, also, the products formation reached a maximum. The concentration of acetophenone and 1-phenylethanol increases up to 6 h and, on further illumination, 1-phenylethanol decreases with an increase of acetophenone under the same conditions. This behavior can be explained by the dehydration of 1-phenylethanol after the subsequent attack of hydroxyl radicals and is discussed in a later section of this paper.

Effect of EB concentration

In photocatalytic reactions, the observed rate constant decreases with the increase of initial substrate concentration. The main steps during the photocatalytic reaction occur on the surface of the catalyst, and, therefore, a high adsorption capacity is associated, favoring the reaction. It is assumed that most of the reactions follow a Langmuir–Hinshelwood kinetic rate model, which means that, for high initial concentrations, all catalytic sites are occupied. A further increase of the concentration does not affect the actual catalyst surface-covered amounts, and, therefore, this may result in a decrease of the observed rate constant. The effect of substrate

Table 2 Solar photocatalytic conversion of EB over: (1) P25 and TCNS (wt%), (2) TCNS0, (3) TCNS1, (4) TCNS3, (5) TCNS5, (6) TCNS10, (7) TCNS15, (8) TCNS25, (9) TCNS40 doped TiO_2 catalysts

Catalyst	Conversion of ethylbenzene (%)	Yield of acetophenone (%)	Yield of 1-phenylethanol (%)	Others (% yield)[a]
TiO_2 P25	42.3	14	10	18.3
TCNS0	41	16	6	19
TCNS1	40.1	23.7	14.1	2.3
TCNS3	42.5	25.3	13.6	3.6
TCNS5	56.1	33.4	21.7	1.0
TCNS10	51.9	28.5	17.8	5.6
TCNS15	50.3	17.8	8.5	24
TCNS25	48.9	28.5	18.2	2.2
TCNS40	45.4	20	11.7	13.7

Reaction conditions: P = air 1 atm; T = 35 °C; irradiation time = 6 h; catalyst amount: 3.3 g L^{-1}; illumination = solar light; EB: H_2O = 5.4

[a] Benzaldehyde, benzoic acid, reductive dimerized products of benzaldehyde, acetophenone

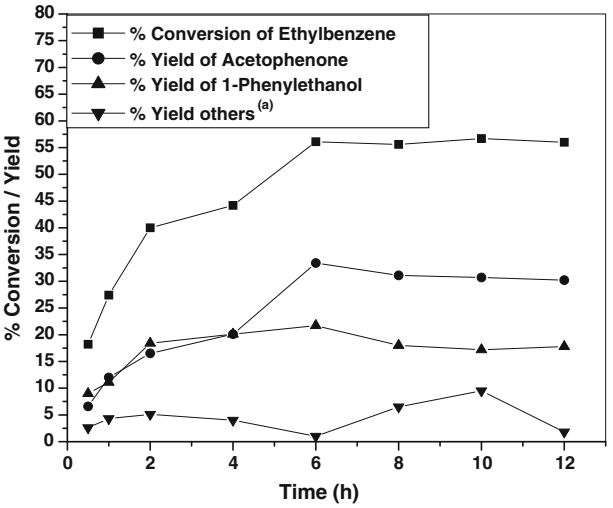

Fig. 4 Conversion of EB time course during the oxidation over TCNS5. Reaction conditions: P = air 1 atm; T = 35 °C; irradiation time = 6 h; catalyst amount: 3.3 g L^{-1}; illumination = solar light; EB: H_2O (molar) = 5.4. [a]Benzaldehyde, benzoic acid, and diols

concentration is an important parameter for the photocatalytic conversion of EB over known catalyst amounts. The concentrations of 0.34–16.38 ($\times 10^{-2}$ M) EB are studied over TCNS5 catalyst with 3.33 g L^{-1} catalyst amount. It is seen from the observed data (Table 3) a decreasing trend in the conversion of EB when the initial concentration is increased for the oxidation reaction. The concentration of 2.73×10^{-2} M shows a maximum conversion and yield compared to other concentrations. This indicates that it is optimum and, at higher concentrations, the OH radicals produced by the catalyst are not sufficient to oxidize the EB molecules which are adsorbed or near the catalyst surface. Hence, 2.73×10^{-2} M solution is chosen for the oxidation, as there is an equilibrium between the adsorption of reactant molecules and the generation of OH radicals from the active sites. The concentration of EB below 2.73×10^{-2} M is converted into fragmented products like benzoic acid, benzaldehyde, and benzene. When the concentration of EB is greater than 2.73×10^{-2} M, 1-phenylethanol is converted into acetophenone which, is further undergoing transformation as a reductive dimerized product like 2,3-diphenyl-2,3-butanediol.

Effect of catalyst amount

In photocatalytic processes, the initial rates of reaction are found to be proportional to the amount of catalyst. However, above a certain quantity, the reaction rate becomes independent of the amount of catalyst. This limit corresponds to the maximum amount of TiO_2 at which all particles are totally illuminated. In order to avoid an ineffective excess amount of the catalyst and to ensure a total absorption of efficient photons on the surface, the optimum amount of catalyst has to be found.

Table 3 Effect of EB concentration over TCNS5 for photocatalytic oxidation

EB concentration ($\times 10^{-2}$ M)	Ethylbenzene (% conversion)	Acetophenone (% yield)	1-phenylethanol (% yield)	Others (% yield)[a]
0.34	81.8	36.4	8.3	37.1
0.68	76.4	40.2	8.6	27.6
1.36	60	22.3	9.7	28
2.73	56.1	33.4	21.7	1
4.09	45.5	22.2	13.7	10
5.46	42.2	21.3	12.9	8
10.92	42	19.2	1	20
16.38	39.5	18.3	1.5	19.7

Reaction conditions: P = air 1 atm; T = 35 °C; irradiation time = 6 h; catalyst: 3.3 g L^{-1}; illumination = solar light; EB: H_2O (molar) = 5.4

[a] Benzaldehyde, benzoic acid, and diols

The data obtained in Table 4 illustrates the effect of variable activity of the TCNS versus the catalyst quantities of 1.66, 3.33, 4.99, and 6.66 g L^{-1} in the suspension. It is observed that, increasing the catalyst amount from 1.665 to 3.33 g L^{-1}, the photocatalytic activity has increased, and at higher amounts, the activity trend is not encouraging and the higher quantities of the catalyst makes the solution turbid, which obstructs the light path into the solution and, in turn, reduces the formation of OH radicals. In the present study, 3.33 g L^{-1} is found to be the optimum catalyst amount for the efficient oxidation of EB.

Effect of oxygen

The presence of an electron acceptor is essential in order to enhance the separation of photo-generated electrons and holes, improving the efficiency of the photocatalytic process. We attempted to discover the influence of oxidation with air, molecular oxygen, and nitrogen on EB oxidation. Air seems to be the more suitable oxidant than molecular oxygen Table 5. The continuous flow of air or molecular oxygen does not improve the extent of mild oxidation, but it leads to total oxidation,

Table 4 Effect of TCNS catalyst amount on the solar photocatalytic oxidation of EB

Catalyst (g $L^{-1)}$)	Ethylbenzene (% conversion)	Acetophenone (% yield)	1-phenylethanol (% yield)	Others (% yield)[a]
1.66	54.25	8	15.5	12.7
3.33	56.1	33.4	21.7	1
4.99	53.6	26.3	0.2	27.1
6.66	52.9	26.9	0.2	25.8

Reaction conditions: P = air 1 atm; T = 35 °C; irradiation time = 6 h; illumination = solar light; EB: H_2O (molar) = 5.4

[a] Diols, benzaldehyde, and benzoic acid

like in any degradation/mineralization that occurs during photocatalytic treatment. However, in the absence of an electron acceptor, the recombination of the electron–hole pairs is very fast, inhibiting the photocatalytic process as observed from the results obtained during N_2 bubbling. The role of oxygen is discussed in the reaction mechanism part. Dissolved oxygen is strongly electrophilic and, thus, an increase of its content probably reduces unfavorable electron–hole recombination routes. However, higher concentrations lead to a downturn of the reaction rate, which can be attributed to the fact that the TiO_2 surface becomes highly hydroxylated, inhibiting the adsorption of substrate at the active sites [26]. Another point to make from the XRD data [11], only anatase phase and no rutile phase is observed. The increase in the oxidation of EB could be due to the oxygen-adsorbed capacity over the TCNS catalyst, which contains only anatase. A further point to mention here is that the rutile phase possesses a lower capacity to adsorb the oxygen than the anatase phase [27]. In our study, the lesser activity of P25 is observed probably because P25 is a combination of anatase and rutile.

Optimization of the EB:H_2O molar ratio

The investigation of water molecules for h^+ scavenger in the presence of molecular oxygen is illustrated. An interesting observation is that irradiation with solar light provided high selective hydroxylation at the α-carbon to the benzene ring in EB. The ratio of EB to water is evaluated in order to discover the role of water during selective oxidation of the present substrate. The hydroxyl radicals generated from water are thought to be attacked on α-carbon of the benzene ring than β-carbon in EB. Molecular oxygen would be reduced by the photoexcited electron to form a nucleophilic oxygen species such as superoxide. It is believed that some kind of active oxygen would be generated in these photocatalytic oxidation systems, such as superoxide, hydrogen peroxide, and hydroxyl radical, which would provide high selectivity. For the direct and selective oxidation of the methylene group in EB, selective generation of electrophilic active oxygen species in the system would be important. This investigation resulted in the observation that undesirable oxidation of side chains reduces the selectivity when we employ molecular oxygen and water as an oxidant in sunlight irradiation. It can be seen clearly from Table 6 that, when the molar ratio of EB to water increases, the conversion of EB is increasing and at the particular ratio 5:4, the formation of acetophenone is found to be the highest.

Table 5 Influence of air/O_2/N_2 on EB oxidation

Oxidant	Ethylbenzene (% conversion)	Acetophenone (% yield)	1-phenylethanol (% yield)	Others (% yield)[a]
N_2	2.0	0.5	–	1.5
O_2	58.0	32.0	19.5	6.5
Air	56	33.4	21.7	1.0

Reaction conditions: P = air/O_2/N_2 1 atm; T = 35 °C; irradiation time = 6 h; catalyst: 3.3 g L^{-1}; illumination = solar light; EB: H_2O (molar) = 5.4

[a] Benzaldehyde, benzoic acids, and diols

Further increase of water leads to total oxidation. It is speculated that EB is adsorbed on the catalyst surface, radicals are generated at the methylene carbon, with subsequent loss of a proton, and it attacks the hydroxyl forms in 1-phenylethanol. The process continues until further attack of hydroxyl at the methylene carbon. As two hydroxyl groups are existing on the same carbon, it loses a water molecule in order to attain a stable state that leads to the formation of acetophenone product.

Effect of particle dimensions and surface area

The lower photocatalytic activity of P25 (TiO_2) compared with the lab-made sample is clearly shown in Table 2. This can be attributed to particle size and the surface area of P25 (TiO_2) and TCNS0. Though the particle size of TCNS0 is less compared to P25, the activity of EB oxidation is appreciable. This can be attributed to its solar harvesting property compared to the P25 sample. Also from Table 1, the observed higher activity of TCNS5 when compared with other CNS wt% loaded TiO_2 catalysts are due to their particle size and surface area. Particle size and, ultimately, particle dimensions are responsible for the photoactivity of the semiconductor, since the electron–hole recombination process was shown to be particle size-dependent [28]. P25 (TiO_2) is found to be less active for EB oxidation under solar light illumination. It is known that, in the nanometer-size range, the physical and chemical properties of the semiconductors are modified when compared to bulk size dimensions [29].

The particle size of 4.6 nm is found to be the optimum in the present case, and any further reduction in size seems to decrease the activity, as is seen from Table 2. Small variations in particle size leads to greater modifications in surface/bulk ratio properties, thus, modifying the significance of volume and surface electron–hole recombination processes. Generally, it is assumed that the lesser size the particle (in a nanometer range), the higher the efficiency of the photocatalytic process. However, if the TiO_2 particle size is extremely reduced, in the range of a few nanometers, lattice defects can lead to an increase in the electron–hole recombination.

Additionally, particle size is an important parameter for heterogeneous catalysis in general, since it directly impacts the specific surface area of a catalyst. The number of active surface sites increases with smaller particles and that results

Table 6 Effect of the EB:water molar ratio for photocatalytic oxidation over TCNS5 catalyst

Molar ratio of EB:H_2O	Ethylbenzene (% conversion)	Acetophenone (% yield)	1-phenylethanol (% yield)	Others (% yield)[a]
1.36	21.5	11.8	4.9	4.8
2.71	35.7	17.2	5.3	13.2
4.05	46.8	22.6	7.9	16.3
5.40	56.1	33.4	21.7	1.0
6.76	47.5	20.1	8.7	18.7

Reaction conditions: P = air 1 atm; T = 35 °C; irradiation time = 6 h; catalyst amount: 3.3 g L^{-1}; illumination = solar light

[a] Benzaldehyde, benzoic acid, benzene, and diols

in a higher rate of the photocatalytic reaction. Some studies revealed that the photocatalytic efficiency does not monotonically increase with decreasing particle size and that there exists an optimal particle size of a few nanometers (3–10 nm) for pure nanocrystalline TiO_2 photocatalyst [30]. Though high thiourea loadings improved the surface area, it has shown a detrimental effect in EB oxidation. These observations are evident from Tables 1 and 2. The surface area of a solid catalyst is directly related to the concentration of active sites for the adsorption and reaction. A large surface area can be a determining factor in certain photocatalytic reactions, since the adsorption of large mounts of substrate and oxygen promotes the reaction rate. However, powders with high surface areas are usually associated with large amounts of crystal lattice defects, facilitating the recombination of the photogenerated electron–hole pairs, leading to a poor photocatalytic activity. It has been reported that the photocatalytic activity of amorphous titanium dioxide is negligible, indicating that crystallinity is an important requirement. Therefore, a balance between surface area and crystallinity must be reached in order to obtain the maximum photoactivity.

Effect of pH

The effect of pH is an important parameter because it commands the surface charge properties of the catalyst and, therefore, the adsorption of the EB. The pH studies at 5–10 are carried over TCNS5 catalyst. The adsorption capacity of the catalyst in different pH ranges is not very much affected due to the non-ionic nature of EB. The results depicted in Table 7 show that, at the original pH, the conversion of EB is more or less the same compared to acidic or basic medium. This may be due to the non-ionic nature of EB. In basic medium, there is a slight increase in 1-phenylethanol and this is observed when compared to the acidic medium. This may be because the OH radicals groups and the hydroxylation at alpha carbon to the benzene in EB, as well as in 1-phenylethanol, is clearly favored with an increase in pH, whereas in acidic medium, such hydroxylation is not favored.

Catalyst recycling studies

To confirm the advantage of the present heterogeneous TCNS5 photocatalyst in the liquid-phase oxidation process, we have reused the catalyst after separation from the

Table 7 Effect of pH for the oxidation of EB over TCNS5 photocatalyst

pH	Ethylbenzene (% conversion)	Acetophenone (% yield)	1-phenylethanol (% yield)	Others (% yield)[a]
5	55.5	23.9	15.5	16.1
10	55.5	24.9	19.5	11.1
7	56.1	33.4	21.7	1.0

Reaction conditions: P = air 1 atm; T = 35 °C; irradiation time = 6 h; catalyst amount: 3.3 g L^{-1}; illumination = solar light

[a] Benzaldehyde, benzoic acid, and diols

Table 8 Recycle studies on photocatalytic oxidation of EB over TCNS5

Cycles	Ethylbenzene (% conversion)	Acetophenone (% yield)	1-phenylethanol (% yield)	Others (% yield)[a]
1	56.1	33.4	21.7	1
2	55	32	20	5
3	54	31	21	2

Reaction conditions: P = air 1 atm; T = 35°C; irradiation time = 6 h; catalyst amount: 3.3 g L^{-1}; illumination = solar light

[a] Benzaldehyde, benzoic acid, and diols

reaction mixture followed by washing with acetonitrile while avoiding the loss of catalyst particles. The results of reusability of the best catalyst are provided in Table 8. After completion of the first cycle, the catalyst is recovered, dried, and reused as such (without any calcination) for the second cycle. A slight decrease in the conversion of EB is observed compared to the first cycle. When the same catalyst is reused without calcination for the third cycle, a slight decrease in the conversion of EB is observed compared to the first and second cycles.

The difference in activity is due to the accumulated organic intermediates on the surface of the catalyst. These affect the adsorption concentration of the reactant molecules, in turn reducing the activity. This observation is confirmed by calcining the third cycle used sample at 400 °C for 3 h and subjecting it to a fourth cycle activity evaluation. The original activity of the catalyst for EB conversion is restored. This indicates that calcination of the used catalyst is necessary in order to regain the activity. Furthermore, this is substantiated by comparison of the surface characterization studies like SEM analysis (Fig. 2c of used catalyst), XRD (not shown), and UV–Vis DRS techniques on the fresh and third cycle used samples (Fig. 3c). This confirms that the structural features of the TCNS5 did not change during the oxidation. Thus, the above studies prove that the catalyst is reusable for a number of cycles without any loss in activity and is stable for longer life. Based on the results obtained, the following observations are made during EB oxidation with air under soft reaction conditions. It is confirmed that the TCNS5 is stable and reusable in the reaction. In view of this, the following mechanistic steps in the oxidation of EB can be envisaged.

Plausible reaction mechanism

The photoexcitation of the semiconductor produces electrons generated in the conduction band and holes in the valence band of TCNS catalyst on solar light illumination:

$$\mathrm{CNS-TiO_2} \xrightarrow{h\nu} \mathrm{CNS-TiO_2(e^-)_{ad}} + \mathrm{CNS-TiO_2(h^+)_{ad}} \quad (1)$$

The water molecule adsorbed on the surface of the catalyst reacts with the hole, giving hydroxyl radical and a proton:

$$H_2O_{(ad)} - CNS - TiO_2 + h^+ \rightarrow {}^{\bullet}OH + H^+ \quad (2)$$

Oxygen adsorbed on the catalyst surface serves as an electron acceptor for the conduction band electron that gives a super oxide radical anion:

$$CNS - TiO_2(e^-)_{ad} + O_2 \rightarrow CNS - TiO_2 - O_2^{\bullet -}{}_{(ad)} \quad (3)$$

The proton generated in Eq. 2 reacts with the super oxide radical anion in Eq. 3, giving rise to hydrogen peroxide (Eq. 4). This peroxide reacts with the photons, producing two hydroxyl radicals:

$$\begin{gathered} O_2^{\bullet -} + H^+ \rightarrow HO_2^{\bullet} \\ 2HO_2^{\bullet} \underset{-O_2}{\longrightarrow} H_2O_2 \xrightarrow{h\nu} 2{}^{\bullet}OH \end{gathered} \quad (4)$$

Thus, the hydroxyl radicals formed react with the surface hydroxyl of the TiO_2 surface which, in turn, loses a water molecule, resulting in a Lewis basic radical site at the oxygen of the surface hydroxyl of TiO_2. The EB is reacted with Lewis acidic center at the surface of the TiO_2. The subsequent loss of the proton at α-carbon to the benzene in EB by Lewis basic free radical site facilitates to return the TiO_2 into its original form. Thus, the formed EB radical at α-carbon to the benzene in EB reacts with the OH radical to give 1-phenylethanol. At this stage, any further hydroxylation at low EB concentrations leads to the formation of benzaldehyde, benzoic acid, benzene, and traces of reductive dimerized product of benzaldehyde.

The process repeats with hydroxyl radical and subsequent dehydration to form Lewis basic radical on the catalyst surface. The proton at α-carbon to the benzene in 1-phenylethanol reacts with the Lewis basic radical site, facilitating abstraction of the proton from α-carbon to the benzene in 1-phenylethanol and, in turn, attacked by hydroxyl radical to form dihydroxy α-carbon. At this stage, to attain the stability of dihydroxy carbon, it loses a water molecule to form acetophenone releasing back the TiO_2 in its original form. The acetophenone formed can also undergo reductive dimerization to form 2,3-diphenyl-2,3-butanediol, as depicted in Scheme 2. All of the products are confirmed with mass and NMR spectroscopy and compared with authentic samples.

Conclusions

The present study demonstrates C, N, and S doped TiO_2 photocatalyst activity for EB oxidation. The results conclude that 5 wt% thiourea doped TiO_2, i.e., TCNS5, is an efficient catalyst and the high activity and selectivity may be due to the high surface area, lower electron–hole recombination, and the stronger adsorption in the visible light region. The substrate concentration of EB of 2.73×10^{-2} M, catalyst amounts 3.33 g L^{-1}, and a neutral pH are found to be favorable conditions for higher oxidation rates. The catalyst activity is found to be sustainable even after the third cycle (as evidenced by SEM, XRD, and UV–Vis DRS techniques). In summary, the application of photocatalytic oxidation of EB offers a step forward in sustainable catalysis. This is advantageous from the standpoint of low cost,

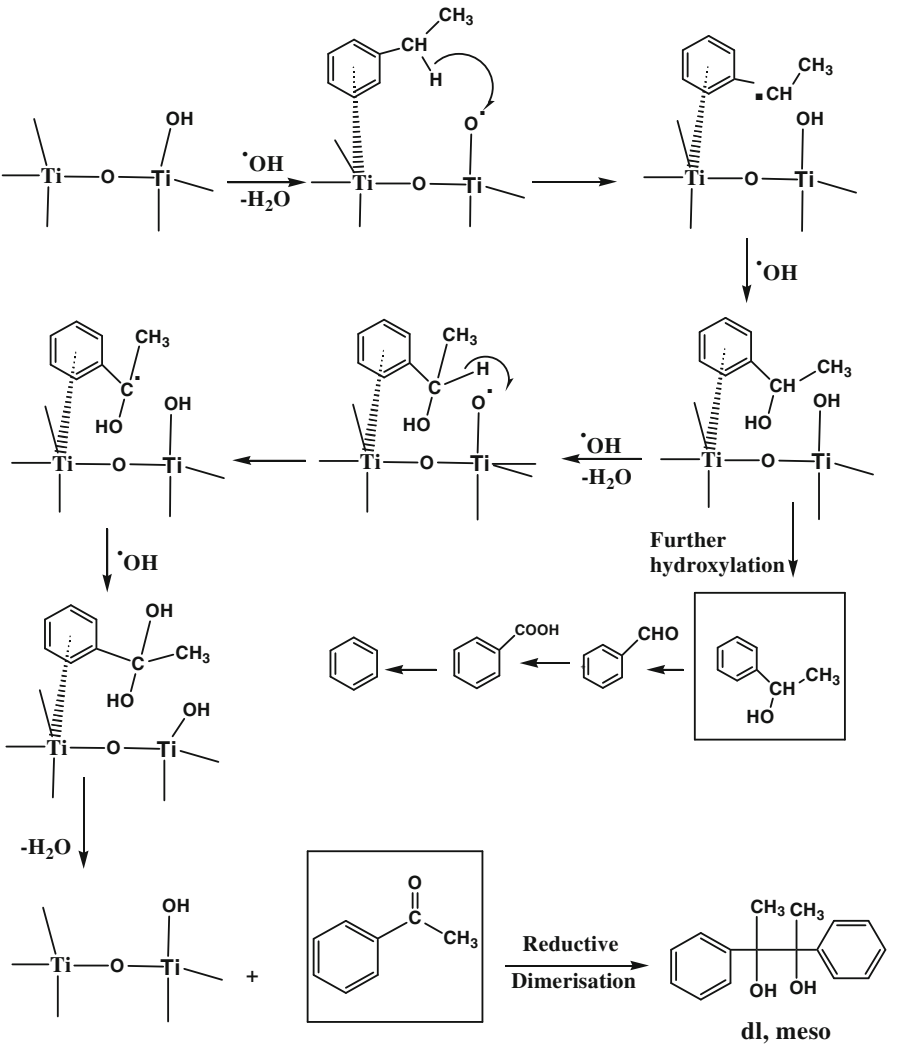

Scheme 2 A plausible reaction mechanism for EB oxidation over TCNS photocatalyst

environmentally friendliness, and operational simplicity, and it may be applicable to large-scale reactions with further fine tuning of the system.

Acknowledgments The authors P.A.K.R. and M.S. thank the Council of Scientific and Industrial Research (CSIR) (New Delhi, India) Emeritus Scientist Scheme.

References

1. P.P. Toribio, A. Gimeno-Gargallo, M.C. Capel-Sanchez, M.P. De Frutos, J.M. Campos-Martin, J.L.G. Fierro, Appl. Catal. A **363**, 32–39 (2009)

2. P.S. Singh, K. Kosuge, V. Ramaswamy, B.S. Rao, Appl. Catal. A **177**, 149–159 (1999)
3. C. Guo, Q. Peng, Q. Liu, G. Jiang, J. Mol. Catal. A **192**, 295–302 (2003)
4. H. Ma, J. Xu, Q. Zhang, H. Miao, W. Wu, Catal. Commun. **8**, 27–30 (2007)
5. S.K. Jana, Y. Kubota, T. Tatsumi, J. Catal. **247**, 214–222 (2007)
6. V.R. Choudhary, J.R. Indurkar, V.S. Narkhede, R. Jha, J. Catal. **227**, 257–261 (2004)
7. K.V. Subba Rao, B. Srinivas, M. Subrahmanyam, in *Photo/Electrochemistry & Photo Biology in the Environment, Energy and Fuel*, ed. by S. Kaneco, B. Viawanathan, K. Funasaka (Research Signpost, Trivendrum, 2004), p. 31–89
8. G. Palmisano, V. Augugliaro, M. Pagliaro, L. Palmisano, Chem. Commun. **33**, 3425–3427 (2007)
9. A. Maldotti, A. Molinari, R. Amadelli, Chem. Rev. **102**, 3811–3836 (2002)
10. O. Carp, C.L. Huisman, A. Reller, Prog. Solid State Chem. **32**, 33–117 (2004)
11. P. Anil Kumar Reddy, P.V. Laxma Reddy, M. Sharma, B. Srinivas, V. Durga Kumari, M. Subrahmanyam, J. Water Resour. Prot. **2**, 235–244 (2010)
12. J. Madarasz, A. Braileanu, G. Pokol, J. Anal. Appl. Pyrolysis **82**, 292–297 (2008)
13. X. Chen, S.S. Mao, Chem. Rev. **107**, 2891–2959 (2007)
14. W. Ho, J.C. Yu, S. Lee, Chem. Commun. **10**, 1115–1117 (2006)
15. M. Carraro, M. Gardan, G. Scorrano, E. Drioli, E. Fontananova, M. Bonchio, Chem. Commun. **43**, 4533–4535 (2006)
16. M.H. Habibi, A.Z. Isfahani, A. Mohammadkhani, M. Montazerozohori, Chem. Monthly **135**, 1121–1127 (2004)
17. J. Geng, D. Yang, J. Zhu, D. Chen, Z. Jiang, Mat. Res. Bull. **44**, 146–150 (2008)
18. Y. Li, C. Xie, S. Peng, V. Lub, S. Li, J. Mol. Catal. A **282**, 117–123 (2008)
19. S. Sakthivel, M. Janczarek, H. Kisch, J. Phy. Chem. B **108**, 19384–19387 (2004)
20. Y. Yokosuka, K. Oki, H. Nishikiori, Y. Tatsumi, N. Tanaka, T. Fujii, Res. Chem. Int. **35**, 43–53 (2009)
21. F. Dong, W. Zhao, Z. Wu, Nanotechnology **19**, 365607–365611 (2008)
22. C. Gopinath, J.Phys. Chem. B **110**, 7079–7080 (2006)
23. J.A.R. Herrera, K. Pierzchała, A. Sienkiewicz, L. Forro, J. Kiwi, J.E. Moser, C. Pulgarin, J. Phys. Chem. C **114**, 2717–2723 (2010)
24. Y. Amour, H.K. Shon, I.J. El Saliby, R. Naidu, J.B. Kim, J.H. Kim, Biosource Technol. **101**, 1453–1458 (2010)
25. A. Zaleska, Physicochem. Probl. Miner. Process. **42**, 211 (2008)
26. A.M. Braun, M.T. Maurette, E. Oliveros, in *Photochemical Technology*, ed. by J.W. Sons (Wiley, Chichester, 1991), p. 397
27. Z. Zhang, C. Wang, R. Zakaria, J.Y. Ying, J. Phys. Chem. B **102**, 10871–10878 (1998)
28. M. Herrmann, Top Catal. **34**, 499–505 (2005)
29. X. Li, X. Quan, C. Kutal, Scripta Mater. **50**, 499–505 (2004)
30. B. Ohtani, Y. Ogawa, S. Nishimoto, J. Phys. Chem. B **101**, 3746–3752 (1997)